Solar Energy 255 (2023) 208–221

Contents lists available at ScienceDirect

Solar Energy

journal homepage: www.elsevier.com/locate/solener

The value of forecasts for PV power plants operating in the past, present and future Scandinavian energy markets

Øyvind Sommer Klyve [a,b,*], Magnus Moe Nygård [a], Heine Nygard Riise [a], Jonathan Fagerström [a], Erik Stensrud Marstein [a,b]

[a] Department for Solar Power Systems, Institute for Energy Technology (IFE), 2007 Kjeller, Norway
[b] Department of Technology Systems, University Of Oslo (UiO), 2007 Kjeller, Norway

ARTICLE INFO

Keywords:
Day-ahead market
Intraday market
Imbalance settlement
PV power forecasting
Market integration

ABSTRACT

When participating in the Scandinavian wholesale energy markets with intermittent PV power, imbalances between market-committed and actual energy generation need to be economically accounted for in the imbalance settlement. The market-committed energy is based on forecasts issued at specific timestamps defined by the market. The economic value of such forecasts can be quantified for the past, present and future energy market regulations by comparing the achieved income using perfect forecasts to the income with imperfect forecasts. Differences between these regulations include changing from 60 min to 15 min market intervals, and from a dual-price to a single-price imbalance settlement structure.

PV power production data were modelled from meteorological measurements carried out at 11 locations in each of the Nord Pool bidding areas. Forecasts generated from a smart persistence model and a more sophisticated numerical weather prediction (NWP) model were compared for these locations, and the value of these forecasts was estimated from historical market data for each of the 11 bidding areas. The results show that the estimated income, and income losses, are dependent on the electricity mix of the bidding areas. In addition, the transition from the dual-price to the single-price imbalance settlement structure reduces the value of providing accurate forecasts. Moreover, the added incentive to provide accurate forecasts when settling the markets and imbalances on 15 min instead of 60 min intervals is negligible with the single-price imbalance settlement. Finally, the results show that intraday trading is generally beneficial for PV power plants in Scandinavia.

1. Introduction

Due to the rapid cost reduction of PV technology, utility scale PV power plants are entering the Scandinavian energy markets. Currently, only onshore wind is cheaper than PV power plants when considering the average Levelized Cost of Energy (LCOE) for new investments of generating units in Sweden (Energiforsk, 2021). In Scandinavia, most of the electricity consumption is cleared in the energy markets organized by Nord Pool. The day-ahead market is, for instance, clearing around 90% of the total power consumption in the Nordic countries (Micic, 2022). In order to participate in the markets, the PV producers must respect given market gate closures, and thus, these timestamps are well-defined deadlines for issuing forecasts. By providing inaccurate forecasts, imbalance between market-committed energy and actual energy generation is introduced into the market. Such imbalances have to be economically accounted for in the imbalance settlement post-operation.

Several works have investigated the value of Variable Renewable Energy (VRE) forecasts in different day-ahead markets throughout the world. Pierro et al. (2020) estimated the energy generation of 1325 synthetically modelled PV power plants across Italy based on satellite data on hourly resolution. Using historical market data, the authors demonstrate how inaccurate forecasts can generate higher income than perfect forecasts in some regions under the single-price imbalance settlement. De Giorgi et al. (2015) investigated the accuracy of different forecasting techniques under five forecast horizons ranging from 1 h to 24 h. The results were used to investigate the performance of the forecast in a modelled Italian day-ahead market and it was found that the most accurate forecast maximized the revenues. For the Spanish day-ahead market, Antonanzas et al. (2017) investigated the economic value of different forecast techniques relative to a persistence forecast. They found that all proposed forecasting techniques that were more accurate than the persistence forecast achieved a higher profit than the

* Corresponding author at: Department for Solar Power Systems, Institute for Energy Technology (IFE), 2007 Kjeller, Norway.
E-mail address: oyvind.klyve@ife.no (Ø.S. Klyve).

https://doi.org/10.1016/j.solener.2023.03.044
Received 30 August 2022; Received in revised form 16 February 2023; Accepted 21 March 2023
Available online 28 March 2023
0038-092X/© 2023 The Author(s). Published by Elsevier Ltd on behalf of International Solar Energy Society. This is an open access article under the CC BY license (http://creativecommons.org/licenses/by/4.0/).

persistence forecast when considering the Iberian market prices and dual-price imbalance settlement scheme. Moreover, it was concluded that their most accurate forecast maximizes the profits. Luoma et al. (2014) calculated the forecast value for 63 modelled PV power plants using day-ahead forecasts generated by the North American Mesoscale (NAM) numerical weather prediction model. The imbalances were settled in the real-time market, and their results demonstrate that biased forecast can achieve higher income than non-biased forecasts. Nevertheless, it was found that a perfect forecast will maximize the revenues of the PV power plant. Wang et al. (2022) compared the performance of a persistence forecast to the NAM model by calculating the costs of forecast errors for 667 PV power plants across five Independent System Operators (ISO) in the USA using historical day-ahead and real-time market prices. Their results show that the yearly average forecast error cost never surpasses 1.5 $/MWh. In addition, the results indicate that areas with higher PV penetration also have higher imbalance costs. Similar results were found in Spodniak et al. (2021) exploring the influence of wind forecast errors in Denmark, Sweden and Finland on the price spread between the day-ahead, intraday and regulating prices in the Scandinavian energy market. The results show that in bidding areas with larger shares of wind power, e.g., DK1, DK2, and SE4, the wind forecast errors have an influence on the spread between the day-ahead and regulating price, in other words increasing the cost of imbalances under a dual-price imbalance settlement structure. Kaur et al. (2016) investigated the need of flexibility reserves under different PV forecast resolutions and horizons and found that allowing the power plants to operate at shorter time horizons reduces the need of power reserves.

Numerous approaches that depend on a wide variety of different inputs have been suggested for forecasting the energy generated from PV power plants (Antonanzas et al., 2016; Sobri et al., 2018; Chu et al., 2021). Numerical Weather Prediction (NWP) models estimate meteorological variables, such as solar irradiation, but are computationally expensive, and therefore, mainly applicable for the temporal horizons of hours and spatial resolutions of kilometres. Similarly, techniques that depend on satellite images are limited by the issuing frequency and spatial resolution of the satellite which is typically 5–15 min and a few hundred metres. For data-driven methods that rely on time-series of exogenous data, such as meteorological measurements, or endogenous data from the PV power plants, or local sensing techniques using sky images, the spatial and temporal resolution is limited by the frequency of the data-logger and the spatial distribution of the sensors. Thus, very high resolutions can be achieved, but this requires a significant capital and operational expenditure.

This study investigates the expected cost of issuing inaccurate forecasts in the Scandinavian energy markets, i.e., the value of the forecasts for the power producers. Moreover, as the energy market and imbalance settlement structures are in an ongoing transition, we also investigate how the past, present and future structures impact the value of the forecast and incentive for producers to provide accurate forecasts. To achieve this, we make use of three different methods to forecast the energy from the PV power plants. The first method is based on a smart persistence model which is a simple technique where the solar irradiation is assumed to persist over the forecast horizon while accounting for its well-known seasonal and diurnal variation. Despite its simplicity, the technique is efficient, especially for shorter temporal horizons, and therefore, it is often used as a benchmark for other, more complex forecasting techniques (Marquez and Coimbra, 2013). Thus, the forecast generated from the smart persistence approach can be considered as a lower limit with respect to the accuracy of the different, applied forecasts. For the second method, we include a state-of-the-art NWP-based method, i.e., the Integrated Forecasting System (IFS) by the European Centre for Medium-Range Weather Forecasts (ECMWF). Finally, perfect forecast is considered, which under the assumption that there is no bias in the market represents the upper limit of forecast accuracy and value. We make use of historical sub-hourly meteorological data to estimate the potential energy generation from 11 synthetic 10 MWp PV power plants across the Scandinavian bidding areas from 2017 throughout 2021. The income and imbalance costs when issuing the forecasts in the day-ahead and intraday market are then estimated from historical market data acquired from Nord Pool (2022b).

To the best of our knowledge, this is the first time the intraday market is considered when estimating the imbalance cost generated from PV energy forecasts. The comparison of costs for different market and imbalance settlement structures is also considered a novelty. The proposed methodology is applicable for other weather dependent generating units which have to issue forecasts.

2. Theory

The value of PV forecast in the Scandinavian wholesale markets depends on the bidding area specific day-ahead, intraday and reserve market prices as well as the imbalance settlement structure. This section provides an overview of the Scandinavian bidding areas, as well as key properties of the energy markets which determine the resulting prices. As a response to the increasing penetration of VRE units and cross-border energy trading, the Scandinavian energy markets and the imbalance settlement structures are currently in transition (NBM, 2022). The past, present and future structures are presented as well as the development of the electricity mix in the different bidding areas from 2017 throughout 2021. The latter is important since this influences the market prices and imbalance settlement costs, and therefore, also the value of the PV forecast.

2.1. Bidding areas

In the Scandinavian wholesale markets, the countries are divided into bidding areas as shown in Fig. 1 . The local Transmission System Operator (TSO) is responsible for defining the bidding areas, and the goal is to ensure that the power flows and energy prices consider inter-area congestions as the power cannot flow freely throughout the market. The division also ensures lower prices in areas with oversupply of energy, and vice versa, incentivizing the market to balance itself over time (Nord Pool, 2022a).

2.2. Day-ahead market

In the day-ahead market, the energy price for the participating consumers and producers is calculated. Nord Pool is a Nominated Energy Market Operator (NEMO) in Scandinavia and is the designated operator of the day-ahead market (All NEMO Committee, 2022a). The Scandinavian market is coupled with the other European markets and NEMOs through the Single Day-Ahead Coupling (SDAC) where 98.6% of the European Unions (EU) consumption is coupled (All NEMO Committee, 2022b).

Each day before 12:00 CET, the market participants across Europe submit how much energy they will generate or consume for each consecutive hour of the following day and to what price they are willing to sell or buy the energy for. The energy prices and total consumptions are calculated for each hour and each bidding area at the intersection of the aggregated demand and supply curves of the market participants (Nord Pool, 2022a). This is achieved by using the common price coupling optimization algorithm PCR EUPHEMIA (Nord Pool, 2022c). By implicitly auctioning the transmission capacities between the bidding areas in the optimization, the total social welfare is maximized while respecting the cross-border transmission capacities. The generating units are selected by order of merit, meaning the generating units with the lowest marginal operational cost, which is typically wind and solar, are dispatched first. Currently, the day-ahead market is cleared on 60 min intervals. However, before January 1. 2025 the Scandinavian energy market will be cleared on 15 min intervals (Statnett, 2022a).

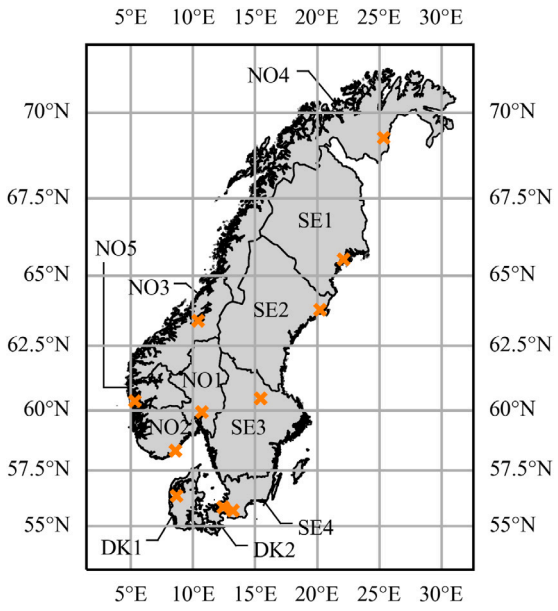

Fig. 1. Map of the Scandinavian bidding areas. The locations of the meteorological stations specified in Table 1 are indicated by the orange markers.

2.3. Intraday market

In case of unforeseen events, such as system faults or weather changes, the market participants can use the intraday market to reschedule their day-ahead contracted production or consumption. As of 2022, the Scandinavian intraday market is organized as a continuous pay-as-bid double auction market, where selling and buying bids are collected, and trades are carried out when there is a buyer and a seller willing to trade for a given price. This is similar to the trading conducted in equity markets (Spodniak et al., 2021). The intraday market opens at 14:00 CET on the day before delivery, and the gate closure is an hour before the start of the specific settlement period. Thus, each settlement period and bidding area might have multiple trades from the intraday market opens until the gate closure. From these trades, a volume weighted average price can be calculated. The Scandinavian intraday market is coupled with European intraday markets by the Single Intraday Coupling (SIDC). In the Scandinavian bidding areas, it is currently only traded 60 min products (All NEMO Committee, 2022c), but there is ongoing work to introduce sub-hourly products, e.g., 15 min products, in addition to intraday auctions (Statnett, 2022a). Nevertheless, the gate closure for the sub-hourly products will still remain an hour before delivery (Statnett, 2022b), i.e., the gate closure for the settlement period 17:30–17:45 CET would be at 16:30 CET. In other European countries, such as Germany and Finland, the intraday gate closure for trades within the bidding area is set up until the beginning of the specific settlement period. In the future, it is possible that this structure might also be introduced in Scandinavia (Statnett, 2022b).

2.4. Regulating power market

During operation, the local TSOs are responsible for ensuring balance in the energy production and consumption to guarantee a stable system frequency. Due to unscheduled events, there might be deviations between the consumption or production compared to what was settled in the day-ahead and intraday markets. Thus, the TSOs need to ensure additional capacity to regulate the energy system during operation.

The TSOs can provide balancing power from owned or leased generating units, or through the Nordic primary, secondary and tertiary balancing reserve markets. The outcome of the manual Frequency Restoration Reserves (mFRR, tertiary reserves) energy market, i.e. the regulating price, is also price setting in the imbalance settlement. In the mFRR energy market, up- and down-regulating bids from producers and consumers are collected up until 45 min before a new settlement period starts. Market participants offering up-regulation are willing to increase production or reduce consumption for a given price. Participants offering down-regulation are on the contrary willing to pay the TSO for reducing production or increasing consumption. During a settlement period, the TSOs activate the required balancing energy bids to maintain the frequency at 50 Hz. The mFRR bids are activated by order of merit, meaning that the producers or consumers with the cheapest bids are dispatched first, and the final activated bid sets the price for all the activated bids within the settlement period. Thus, it should be noted that the regulating price for a settlement period remains unknown until the period has ended. In periods with down-regulation, the up-regulation price is set equal to the day-ahead price, and vice versa. The regulating price might differ between the bidding areas due to transmission congestions.

As the mFRR regulating bids can be changed up until 45 min before the start of a settlement period, the regulating power market has so far been more important than the intraday market in Scandinavia. This is because market participants with flexible generation can offer their imbalances in the regulating market close to dispatch (Spodniak et al., 2021). However, there is no guarantee that the TSO will activate the bids and clear the imbalance, and thus, trading the forecasted imbalance in the intraday market is associated with less risk. The market data show that the intraday and regulating prices have comparable spread around the day-ahead price. This can be seen from the interquartile range of the difference between the intraday and day-ahead prices, and the regulating and day-ahead prices in Table A.1 and Table A.2 in Appendix, respectively. However, the absolute values of the minimum and maximum prices in the regulating market are larger than the ones of the intraday market from 2017 throughout 2021. This is seen for all bidding areas and emphasizes the reduced risk of trading away forecasted imbalances in the intraday market. In this study, it is assumed that the PV power producers do not provide contracted reserves or participate in the regulating market due their inflexible generation. Nevertheless, the regulating price sets the foundation for the cost of production imbalances in the imbalance settlement, and thus, determines the value of the forecast.

2.5. Imbalance settlement

The imbalance settlement in Scandinavia and Finland is carried out by eSett on behalf of the Nordic TSOs. As eSett provides handbooks with detailed descriptions of the imbalance settlement, only a short summary of the imbalance settlement relevant for the study will be given (eSett, 2022b). When there are imbalances between the market-committed energy and the net generation or net consumption within an imbalance settlement period, the market participants are economically accountable for these imbalances. The market participants settle the imbalances with eSett through their Balancing Responsible Party (BRP). Large producers or consumers typically provide their own BRP services, but this service can also be bought from a third party BRP service provider. The BRP is accountable for the net imbalance, i.e., the difference between the market-committed and the actually generated or consumed energy of the producers or consumers in their portfolio within their bidding area. As it is only the net imbalance of the BRP that is settled with eSett, an energy deficit from one power plant in the portfolio of the BRP can be accounted for by an energy surplus from another power plant within the same bidding area. Until November 1. 2021, i.e., during the whole time period of the data collection of this study (except November and December 2021), the imbalance settlement was carried out using the old Nordic Balancing Model (NBM) with a dual-price imbalance settlement. After November 1. 2021, the

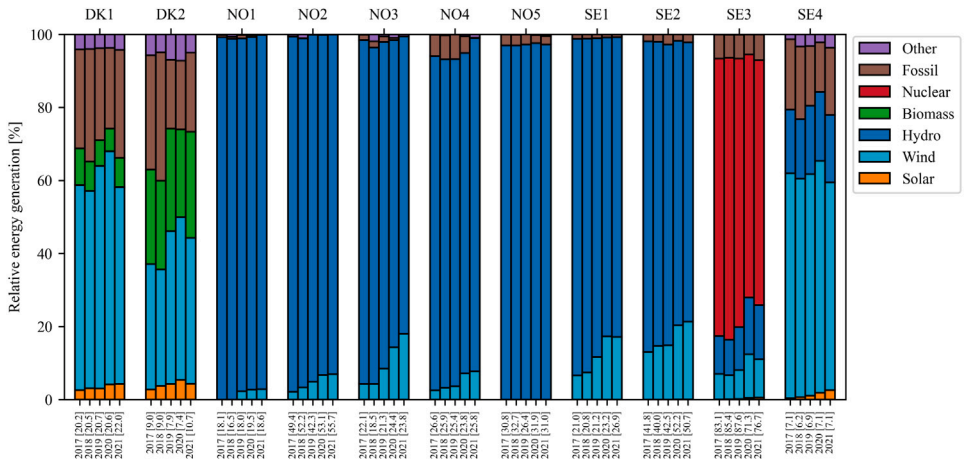

Fig. 2. Electrical energy generation per production type in each of the Scandinavian bidding areas from 2017 throughout 2021. The data for Norway and Denmark were collected from the ENTSO-E Transparency Platform (2022). The Swedish data were collected from the Swedish TSO (Svenska kraftnät, 2022). For the Swedish bidding areas, "Fossil" represents all types of thermal power generation except nuclear. The total generated energy for each year and bidding area is given in TWh in the brackets.

new NBM with a single imbalance price and imbalance fees is in operation. In the present work, the historical prices from the regulating market are used as a basis of both the old and new NBM imbalance settlement.

2.5.1. Old Nordic Balancing Model

In the old NBM with a dual-price imbalance settlement for producers, there is one price for BRPs with an energy deficit and another for BRPs with an energy surplus in their generation in relation to their market commitments (eSett, 2022c). If the TSO activates net up-regulation in a given settlement period and bidding area, the resulting up-regulating price is set from the regulating market, while the down-regulating price is set equal to the day-ahead price. Thus, a BRP with a net energy deficit will have to pay the up-regulating price for its lack of provided energy, but a BRP with a net surplus of energy will only obtain the day-ahead price for its additional energy. Oppositely, when the TSO activates down-regulating bids a BRP with an energy deficit pays eSett the day-ahead price for their deficit, but a BRP with energy surplus will only be paid the regulating market resulting down-regulating price for their additional energy. As the up-regulating price is higher than the day-ahead price, and the down-regulating price is lower, a BRP is always better off when providing a more accurate forecast in the day-ahead market.

2.5.2. New Nordic Balancing Model

In the new NBM, a single-price imbalance settlement structure is used. If the TSO activates net up-regulation for a settlement period, a BRP with an energy deficit has to pay the up-regulating price for the imbalance, but will be paid the up-regulating price if providing an energy surplus. Oppositely, in settlement periods with energy surplus in the energy system, the TSO will activate down-regulation bids. A BRP with an energy surplus is paid the down-regulating price for the additional energy and a BRP with an energy deficit will only have to pay the down-regulating price for the lack of energy. In contrast to the dual-price imbalance settlement, it is possible under the single-price imbalance settlement to achieve higher revenues with an inaccurate forecast than with a perfect forecast. To counteract this possible source of unwanted bias in the market, an imbalance fee was introduced to encourage accurate forecasts. Thus, a BRP providing an imbalance will have to pay an imbalance fee depending on the absolute value of the imbalance. As of August 2022, the imbalance fees are 0.133 €/MWh for the Danish bidding areas and 1.15 €/MWh for the Swedish and Norwegian bidding areas (eSett, 2022a). The new NBM currently has 60 min imbalance settlement periods, but from the end of May 2023, 15 min imbalance settlement periods will be applied (eSett, 2022b).

2.6. Electricity mix and energy prices

The prices in the Scandinavian energy market are dependent on the electricity mix of each bidding area. As seen from Fig. 2, the shares of the total energy generation from wind and solar increased in Scandinavia from 2017 to 2021. The Danish bidding areas (DK1 and DK2) and the southernmost Swedish bidding area (SE4) have the highest shares of wind and solar. Due to the high shares of VRE units in the energy system of these areas, the day-ahead prices are relatively intermittent, as day-ahead prices drop in hours of high wind and solar penetration. In Norway and northern Sweden, hydro power is the main source of electricity, typically providing stable day-ahead prices, but with seasonal and yearly variations depending on the level of precipitation. The hydro reservoir power plants estimate the water value, or alternative cost of producing at a later time, depending on the reservoir filling level and the forecasted market prices (Fosso et al., 1999). Thus, even though there is no fuel cost for hydro power, the market-committed hydro power marginal cost still reflects the overall market prices. For instance, 2020 had much precipitation and the hydro power reservoirs were filled, and thus, the prices dropped across Scandinavia. On the contrary, 2021 had little precipitation and high natural gas prices, and thus, the prices across Scandinavia increased as well, except for the northernmost regions in Sweden and Norway with higher precipitation, but with congestions preventing energy flows from north to south. Hydro power plants also provide efficient regulating power as they are able to ramp at a higher rate than nuclear, biomass, oil, and coal power plants (IEA, 2014).

3. Method

Due to the lack of operating utility-scale PV power plants in some of the Scandinavian bidding areas, energy generated from synthetic PV power plants are modelled using historical meteorological data from different geographical locations. The models used to convert the meteorological data to PV production are given in Section 3.1. The smart persistence forecast technique and the market specific forecast horizons are explained in Section 3.2. Similarly, Section 3.3 explains the forecasts generated by the more advanced NWP model available from ECMWF. In Section 3.4, the assumptions related to the market participation of the modelled PV power plants are given. In Section 3.5, we define three different energy market and imbalance settlement structure cases that has been, or will become operational in Scandinavia. We also include a fourth case with extended gate closure for the intraday market, similar to what is implemented in the German and Finnish intraday markets. Finally, we explain how the revenues, or

Table 1
Location, bidding area, latitude (Φ), longitude (λ), and height above sea level (H) for the meteorological stations where the data used to generate the 10 MW_p synthetic PV power plant output energies were collected. The tilt angles (β) which were optimized for these systems with V5.2 of the PVGIS software are also shown (EU Science Hub, 2022). For all locations, the azimuth angles of the PV modules were set to 180°.

Location	Bidding area	Φ [°N]	λ [°E]	H [m]	β [°]
Mejrup	DK1	56.38	8.67	53	45
Sjælsmark	DK2	55.88	12.41	40	41
Oslo	NO1	59.94	10.72	94	45
Grimstad	NO2	58.33	8.58	–	44
Trondheim	NO3	63.42	10.41	60	44
Iškoras	NO4	69.30	25.35	591	50
Bergen	NO5	60.38	5.33	46	40
Luleå	SE1	65.54	22.11	32	48
Umeå	SE2	63.81	20.24	23	49
Borlänge	SE3	60.49	15.43	168	47
Lund	SE4	55.71	13.21	85	45

rather loss of income due to inaccurate forecasts, are calculated for each of the four cases using historical market data from 2017 throughout 2021.

3.1. Meteorological and synthetic PV energy generation data

Global horizontal irradiance, G, ambient temperature, T_a and wind speed, v, were measured at selected meteorological stations throughout Scandinavia operated by the Danish Meteorological Institute (DMI), the Norwegian Meteorological Institute (MET Norway), and the Swedish Meteorological and Hydrological Institute (SMHI). The measurements were carried out according to the World Meteorological Organization (WMO) standards (WMO, 2019), and historical values are openly available online. The present work made use of data measured at 10 such meteorological stations located in each of the bidding areas in Scandinavia with the exception of NO2 where G was measured by the University of Agder (UiA). The meteorological stations are specified in Table 1 and their locations are also shown in Fig. 1.

In Denmark, G, T_a and v are available as 10 min average aggregate values. For the selected stations in Norway and Sweden, instantaneous values of G are available at 1 min resolution. In NO2, data is only available for 2020 and 2021. Although some stations have T_a and v available as 10 min average aggregate values, others have only 1 h average aggregate values for the entire period between 2017 throughout 2021. Therefore, G, T_a and v are resampled to 15 min average aggregate values to ensure a consistent dataset with 15 min resolution values, corresponding to the 15 min market intervals. The quality of the G data is ensured through application of a quality control filter as given in Eq. (1):

$$4\ \mathrm{W/m^2} < G < \frac{3}{2} G_0 \left(\cos(\theta_z)\right)^{1.2} + 100\ \mathrm{W/m^2} \tag{1}$$

where $G_0 = 1360\ \mathrm{W/m^2}$ is the solar constant and θ_z is the solar zenith angle (Long and Dutton, 2010). For the considered period, less than 3.3% of the 15 min intervals have missing values in either G, T_a, and v when the solar zenith angle is $\theta_z \leq 86.3°$ for all locations apart from NO2 where 4.9% of the data is missing. The v was not measured at the same location as G for the locations in NO2, NO3, NO5, SE1, SE2, SE3 and SE4. Instead, v was measured at another meteorological station typically located less than 3 km away, but for SE2 and SE1 the distance was 8 and 18 km, respectively. For NO2, also the T_a was measured at a meteorological station nearby.

Fig. 3 shows the G and T_a raw-data for NO1 alongside modelled irradiance, temperature and power data for the synthetic 10 MWp PV power plants co-located with the meteorological stations for May 29. 2021. The direct normal irradiance G_{dn} is estimated from the G using the DISC model with a maximum solar zenith angle Max $[\theta_z] = 86.3°$ (Maxwell, 1987). The diffuse horizontal irradiance G_{dh} is obtained from the closure equation:

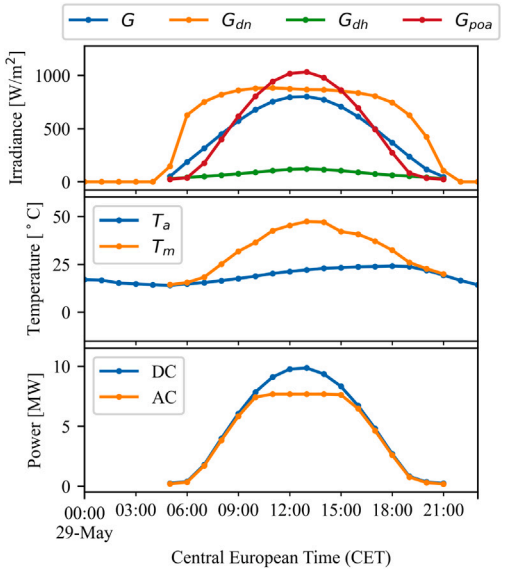

Fig. 3. Measured global horizontal irradiance G and ambient temperature T_a with modelled direct normal irradiance G_{dn}, diffuse horizontal irradiance G_{dh}, irradiance received in the plane-of-array G_{poa}, module temperature T_m, and DC and AC power data for the synthetic 10 MWp PV power plant assumed to be co-located with the meteorological station in NO1 specified in Table 1.

$$G_{dh} = G - G_{dn} \cos\left(\theta_z\right) \tag{2}$$

where θ_z is the solar zenith angle and G and G_{dn} is the global horizontal and direct normal irradiance, respectively. The total irradiance received in the plane-of-array G_{poa} is determined from G, G_{dn}, and G_{dh} for the tilt angles specified in Table 1 using the Perez sky diffuse irradiance model (Perez et al., 1988, 1987, 1990). The module temperature T_m is estimated from T_a and v with the Faiman model (Faiman, 2008). The DC and AC power are modelled with NREL's PVWatts DC power model under the assumption of a DC-to-AC ratio of 1.25 (Dobos, 2014). Finally, the output energy is calculated by the product of the AC power and time interval. It should be noted that snow losses are neglected, i.e., it is assumed that snow is effectively removed from the panels by an operation and maintenance team. The entire modelling workflow was carried out using the pvlib implementation of the models and their default settings unless explicitly stated (Holmgren et al., 2018).

3.2. Smart persistence forecast

The clear-sky index k_t is defined as:

$$k_t = \frac{G_t}{G_{clear,t}} \tag{3}$$

where G_t and $G_{clear,t}$ are the measured and estimated values at clear-sky conditions for the global horizontal irradiance at time t, respectively. In the present work, the pvlib implementation of the Ineichen–Perez clear-sky model is used to estimate the clear-sky irradiance $G_{clear,t}$ (Ineichen and Perez, 2002). In principle, $0 \leq k_t \leq 1$ where $k_t = 1$ indicates completely clear-sky conditions and $k_t = 0$ imply $G_t = 0$. However, $k_t > 1$ is also possible due to scattering of light by the atmosphere and clouds. For this study, it is assumed that Max $[k_t] = 2.0$.

The smart persistence forecast for the global horizontal irradiance $\hat{G}_{t+\Delta t}$ is defined as given in Eq. (4).

$$\hat{G}_{t+\Delta t} = \hat{k}_{t+\Delta t} G_{clear,t+\Delta t} \tag{4}$$

where Δt is the forecast horizon, $\hat{k}_{t+\Delta t} = k_t$, and $G_{clear,t+\Delta t}$ is the estimated clear-sky irradiance at time $t + \Delta t$. When forecasts are to be

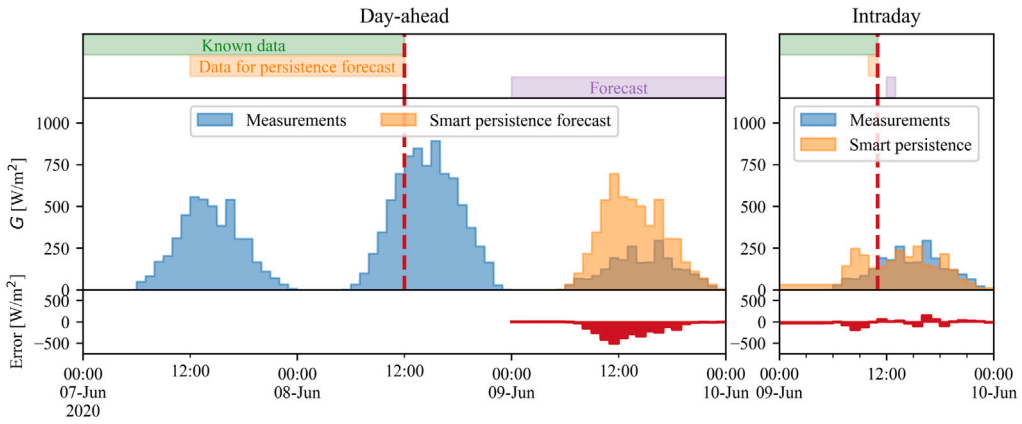

Fig. 4. The present day-ahead (left) and intraday (right) market structure in Scandinavia illustrated for G. The dotted, red line in the left part of the figure highlights the day-ahead market gate closure for the energy to be delivered on June 9. 2020. In the right figure, the red dotted line highlights the intraday market gate closure for the settlement period 12:00–13:00 CET on June 9. 2020. The red bars in the lower part of the figure show the difference between the measured and forecasted energy generation.

issued at night or in periods with missing data, the clear-sky index is not well defined. In these scenarios, the average k_t for the period ±2 h around solar noon on the day before is used. Thus, it is strictly assumed that all periods with missing data are due to scheduled maintenance.

The day-ahead and intraday market structures decide the practicalities of the forecast which are explained for the irradiance forecast on June 9. 2020 in Fig. 4, corresponding to the current market structure with 60 min settling periods. The forecasts were carried out on 15 min resolution before being aggregated to hourly resolution, however, for simplicity the forecasts will be explained as if they were conducted on hourly resolution. As mentioned in Section 2.2, the gate closure for day-ahead production bids is at 12:00 CET the day prior to the day of delivery, thus this would also be the deadline to issue the forecast. This is highlighted by the dashed red line in the left part of Fig. 4. In this study, the day-ahead smart persistence forecast is carried out on the observed k_t of the 24 h leading up to the gate closure. Thus, for the forecasts issued for 00:00 until 11:59 CET $\Delta t = 24$, and for 12:00 until 23:59 $\Delta t = 48$. $\hat{G}_{t+\Delta t}$ is obtained from Eq. (4). Fig. 4 demonstrates that the error can be considerable, especially when there is much variation in the irradiance. Δt is constant and shorter for the intraday forecast with respect to the day-ahead forecast. As a consequence, the intraday smart persistence forecast is more accurate than for the day-ahead equivalent. An example is shown in the right part of Fig. 4, where the deadline for the 12:00–13:00 CET forecast is highlighted by the dashed red line. The final measurements available for the forecast at the indicated deadline, is the data collected in the period 10:00–11:00 CET, such that $\Delta t = 2$ h. Since the data are left binned, $\Delta t = 2$ h means data up to one hour prior to delivery are used to issue the forecast.

The T_a and v are forecasted using a regular persistence forecast, as given in Eq. (5).

$$\hat{X}_{t+\Delta t} = X_t \tag{5}$$

where $X_t = \{T_{a,t}, v_t\}$ is the ambient temperature or wind speed at time t. Here, the same forecast horizons Δt were used as for G. We acknowledge that there is diurnal variation also for T_a and v, but since this variation is not easily modelled we resort to a simple persistence approach.

As explained in Section 3.1, combining the forecasts for G, T_a and v, the day-ahead forecasted energy $\hat{E}_t^{DA}$ and intraday forecasted energy $\hat{E}_t^{ID}$ can be derived for each timestamp. Depending on the different energy market structure cases, Δt for forecasts issued in the day-ahead and intraday market will change. The different values for Δt are highlighted in Table 2.

Table 2
Key features of the defined market cases.

Case	Day-ahead Δt [h]	Intraday Δt [h]	Market/settlement period intervals [h]	Settlement type
1	[24,48]	2	1	Dual
2	[24,48]	2	1	Single
3	[24,48]	1.25	0.25	Single
4	[24,48]	0.25	0.25	Single

3.3. NWP forecast

The Integrated Forecasting System (IFS) by the European Centre for Medium-Range Weather Forecasts (ECMWF) offer operational medium range global weather forecast (Persson and Grazzini, 2007). The high-resolution forecasts (HRES) are issued twice a day, i.e., at 00:00 UTC and 12:00 UTC, providing deterministic forecasted products up until 10 days into the future with an average spatial resolution of ∼ 9 km and a temporal resolution of 1 h. To obtain a forecasted PV power time series, the downwelling short-wave radiation ($ssrd$), the ambient temperature 2 m above ground ($2t$), and the eastward ($u10$) and northward ($v10$) components of the wind at 10 m above ground were obtained for the surface level of the model from the ECMWF Meteorological Archiving System (MARS) for both the 00:00 UTC and 12:00 UTC forecasts for the period from January 1. 2017 to December 31. 2021. Since forecast products may not be available for the exact locations listed in Table 1, we utilize the nearest available forecasts products for the closest grid-point to these locations. The irradiation is given in units J/m^2 as a cumulative sum from the forecast is issued, and therefore, the difference between consecutive forecast products is taken before the time series is multiplied by 3600 s to convert into units of W/m^2. The ambient temperature is given in units K, and therefore, we convert to units °C by subtracting 273.15 K. Finally, the eastward u and northward v component of the wind are given in units m/s and we combine them into a horizontal wind speed by $ws = \sqrt{u^2 + v^2}$. To achieve a 15 min resolution forecast, the available hourly average values are taken as the best estimate for all 15 min values within that hour. CET is either 1 or 2 h ahead of UTC depending on the presence of Daylight Saving Time (DST). To meet the 12:00 CET deadline for the day-ahead forecast, the latest available forecast is generated from the variables forecasted at 00:00 UTC for all market cases. The calculation of the day-ahead forecasted energy $\hat{E}_t^{DA}$ uses the same methodology outlined in Section 3.1. Similarly, the intraday forecasted energy $\hat{E}_t^{ID}$ is generated using the variables forecasted by the latest available forecast at any instance.

3.4. Energy market participation assumptions

When calculating the income from the energy markets, it is assumed that the day-ahead forecasted energy would be dispatched in the market due to the low marginal cost of PV power. We also assume that there is no minimum bid size for the energy offered to the market. Moreover, it is assumed that the energy volumes bid into the markets would not be large enough to have an impact on the final price setting in either of the day-ahead, intraday, or regulating markets. Thus, we assume that the historical market data is valid for the analysis. Finally, it is assumed that the market participants would not change their behaviour under the different modelled market structures, i.e., that the outcome of the price settings would be the same. Complete datasets of historical day-ahead and regulating prices from 2017 throughout 2021 were downloaded from Nord Pools data portal for each bidding area (Nord Pool, 2022b). 98.4% of the intraday prices and traded volumes data were acquired from the data portal. In hours with missing intraday data, it is assumed that no historical trades were recorded. The imbalance fees were extracted from eSetts Data Portal (eSett, 2022a).

During the day of delivery, it is assumed that the producer would use the intraday market to rebid the volumes which were scheduled from the day-ahead market, and by continuously using the updated forecasts to trade on the intraday market from 14:00 CET the day before delivery until the gate closure for the given settlement period. In practice, this is included in the income calculation by assuming the producer achieved the historical volume average intraday price for the given bidding area and settlement period, and that the total energy traded on the intraday market would be the difference between the day-ahead market committed energy and the last issued intraday forecast. However, if there were timestamps with no historical intraday trades in a bidding area, it is assumed that the producers would not have been able to trade either. Intraday auctions are neglected when modelling the future intraday market structures.

Furthermore, it is assumed that each of the modelled PV power plants would be the only power plants with imbalances in the portfolio of their BRP for the given bidding area. Thus, the difference between the market-committed energy and actual energy generation for each PV power plant would be the net imbalance which the BRP would have to settle with eSett. The income losses due to the PV power plant imbalances should as such be considered as an upper bound. This is due to the fact that the BRP could have other power plants in their portfolio for the given bidding area with imbalances in the opposite direction of the PV power plant, reducing the net imbalances and income losses. For the rest of this paper, the PV producers will be autoreferred to as the ones settling the imbalances directly with eSett. For both the old and new NBM, the fixed fees, volume fees, grid tariffs, and peak load reserve fees (in Sweden) are neglected for the income calculations (eSett, 2022b). This is done because they differ between the bidding areas and are irrelevant when assessing the income differences between perfect and imperfect forecasts.

3.5. Energy market structure cases

Four energy market structure cases are defined in order to estimate the value of forecast under the past, present and future energy market and imbalance settlement structures.

3.5.1. Case 1

Case 1 represents the market and settlement structure which was in place in the time period of the data collection, i.e., 2017 throughout 2021 (except for November and December 2021). In this case, there are hourly settlement periods in the markets and imbalance settlement, and the intraday trade gate closure is an hour prior to delivery. The imbalance settlement is carried out with the dual-price model for the whole period disregarding the introduction of the new NBM on November 1. 2021. The income for each PV producer under Case 1 is calculated as given in Eq. (6):

$$\Pi^d = \sum_{t=1}^{T} (\hat{E}_t^{DA} p_t^{DA} + \delta_t (\hat{E}_t^{ID} - \hat{E}_t^{DA}) p_t^{ID} + E_t^{reg} p_t^{reg,d}) \tag{6}$$

where Π^d is the total revenue achieved for the time stamps from $t = 1$ until T in the period from 2017 throughout 2021, $\hat{E}_t^{DA}$ is the day-ahead forecasted and market-committed energy, and p_t^{DA} the spot price for a given bidding area and settlement hour. In settlement periods with historical intraday trades, δ_t is set to 1 and in settlement periods without historical trades δ_t is set to 0. Thus, in settlement periods with historical intraday trades, the difference between $\hat{E}_t^{ID}$ and $\hat{E}_t^{DA}$ is bought or sold in the intraday market to the weighted average price p_t^{ID} of the specific settlement hour and bidding area. The energy imbalance which the system would have to regulate E_t^{reg} is calculated as given in Eq. (7).

$$E_t^{reg} = E_t - \hat{E}_t^{DA} - \delta_t (\hat{E}_t^{ID} - \hat{E}_t^{DA}) \tag{7}$$

For settlement hours without historical intraday trades, the energy imbalance is the difference between the generated energy, E_t, and $\hat{E}_t^{DA}$. Likewise, in hours with historical intraday trades, the energy imbalance is the difference between E_t and $\hat{E}_t^{ID}$. As given in Eq. (8), if the PV power plant has an energy surplus imbalance, i.e., $E_t^{reg} > 0$, the producer is paid the down-regulating price $p_t^{reg,down}$ for this additional energy. Opposite for an energy deficit imbalance, $E_t^{reg} < 0$, the producer will pay the up-regulation price, $p_t^{reg,up}$, for the lacking energy.

$$p_t^{reg,d} = \begin{cases} p_t^{reg,up} & \text{if } E_t^{reg} < 0 \\ p_t^{reg,down} & \text{if } E_t^{reg} > 0 \end{cases} \tag{8}$$

When calculating the perfect forecast income, $\hat{E}_t^{DA} = \hat{E}_t^{ID} = E_t$ such that $E_t^{reg} = 0$.

3.5.2. Case 2

The income under Case 2 is calculated in the same manner as Case 1, but with the new NBM including the single-price imbalance settlement and imbalance fee. Thus, Case 2 corresponds to the present market structure introduced in November 2021. Since the price setting in the regulating power market is the same for both the dual- and single-price imbalance settlement, the historical up- and down-regulating power prices under the dual-price imbalance settlement are used to construct the single regulating price $p_t^{reg,s}$ under the new NBM. This is achieved by setting $p_t^{reg,s} = p_t^{reg,up}$ for operating hours when the system was in up-regulation, and $p_t^{reg,s} = p_t^{reg,down}$ when the system was in down-regulation. The total income under the single regulating price imbalance settlement is calculated as given in Eq. (9):

$$\begin{aligned} \Pi^s = \sum_{t=1}^{T} & (\hat{E}_t^{DA} p_t^{DA} + \delta_t (\hat{E}_t^{ID} - \hat{E}_t^{DA}) p_t^{ID} \\ & + E_t^{reg} p_t^{reg,s} - |E_t^{reg}| p^{fee}) \end{aligned} \tag{9}$$

When calculating the total income under the single-price imbalance settlement Π^s for Case 2, the only difference to Eq. (6) is the inclusion of the imbalance fee p^{fee}, as well as the exchange of the dual to the single regulating price $p_t^{reg,s}$. The energy imbalances are calculated as in Case 1 by Eq. (7).

3.5.3. Case 3

Case 3 represents the market structure which has been decided to be in place by January 1. 2025 with 15 min market and imbalance settlement periods and single regulating prices with imbalance fees. The gate closure for the intraday market would still be an hour prior to delivery, meaning $\Delta t = 1.25$ h. The historical day-ahead, intraday, and regulating power prices on 60 min resolution are modelled with 15 min settlement periods by forward filling the 60 min resolved prices for each of the corresponding 15 min. When calculating the total income under the market structure of Case 3, Eqs. (9) and (7) are used, but with 15 min between each timestamp t.

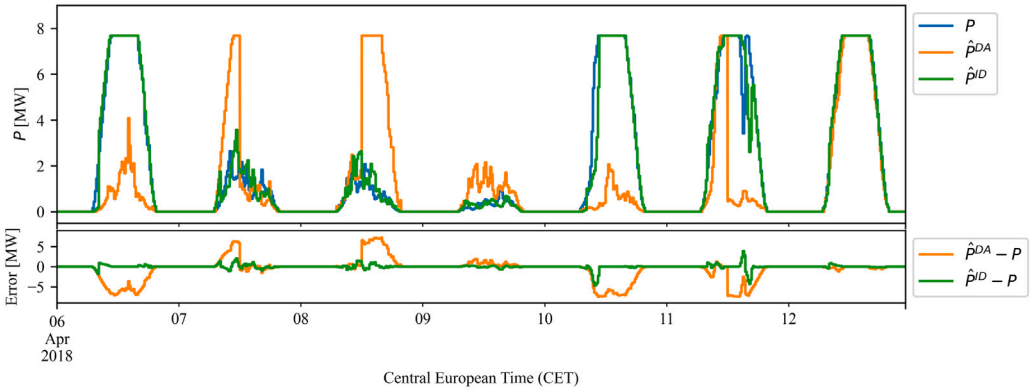

(a)

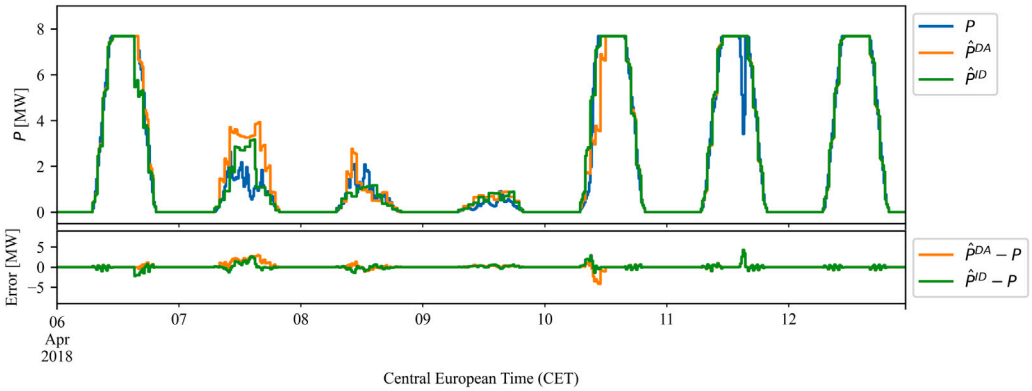

(b)

Fig. 5. Output power P of the synthetic PV power plant in NO1 with day-ahead $\hat{P}^{DA}$ and intraday $\hat{P}^{ID}$ for the smart persistence forecasts (a) and ECMWF forecasts (b) during the period April 6. 2018–April 14. 2018. In both figures, the upper panel shows the 15 min resolution data while the lower panel presents the forecast errors.

3.5.4. Case 4

Case 4 models the proposed market structure after January 1. 2025, but with an extended intraday trading period with gate closures until the start of the delivery period, meaning $\Delta t = 0.25$ h for the intraday forecast. The total income under Case 4 is calculated in the same manner as for Case 3, using Eqs. (7) and (9) on 15 min settlement periods. By repurposing the historical intraday prices, it is assumed that cross-border trades would be possible until gate closure.

4. Results and discussion

4.1. Forecast accuracy

The power outputs of the synthetic PV power plants were generated from the meteorological data as described in Section 3.1. The day-ahead and intraday smart persistence and ECMWF forecasts were carried out as described in Section 3.2 and Section 3.3, respectively. Fig. 5 presents the output power and forecast data during one week in April 2018 for the NO1 location. For this week, the figure exemplifies that the smart persistence intraday forecast is more accurate than the day-ahead counterpart. This is also generally true for the whole analysis period. However, it is also clear that both forecasts can be very accurate during periods with stable weather, *e.g.*, April 12. 2018. The day-ahead forecast is influenced by sampling data from the two prior days. In particular, this can cause the accuracy of the forecast to change abruptly between the morning and afternoon, *e.g.*, April 7. and April 8. 2018. It is also noted that the intraday forecast is less accurate in the morning when the forecast is generated from the average k_t during ±2 h around solar noon on the day before. The day-ahead ECMWF forecast appears more accurate than its smart persistence counterpart. The accuracy seems to improve slightly from the day-ahead forecast with the intraday forecast, but in this case the improvement is much more subtle than for the smart persistence.

To evaluate the accuracy of the forecasts, we consider the mean absolute error $nMAE$ and mean bias error $nMBE$ normalized to the mean energy generation $\bar{E} = \frac{1}{T}\sum_{t=1}^{T} E_t$ defined for a period with T observations in Eqs. (10) and (11):

$$nMAE = \left(\frac{1}{\sum_{t=1}^{T} E_t}\right)\sum_{t=1}^{T}\left|\hat{E}_t - E_t\right| \tag{10}$$

$$nMBE = \left(\frac{1}{\sum_{t=1}^{T} E_t}\right)\sum_{t=1}^{T}\left(\hat{E}_t - E_t\right) \tag{11}$$

where $\{E_t\}_{t=1}^{T}$ and $\{\hat{E}_t\}_{t=1}^{T}$ are the synthetically measured and forecasted output energy, respectively. Here, $\hat{E}_t = \{\hat{E}_t^{DA}, \hat{E}_t^{ID}\}$. Fig. 6 shows $nMAE$ and $nMBE$ calculated for the four different marked scenarios and all the locations in Table 1 during the period 2017–2021. It should be noted that the forecasts are identical in Case 1 and 2.

Fig. 6(a) shows the $nMAE$ and $nMBE$ for the smart-persistence forecast. With this forecast, the mean value among the locations for the day-ahead marked in Case 1 and 2 is $\overline{nMAE} = 0.57$ with a relative absolute difference with respect to $\overline{nMAE}$ below 9% for all the locations. The only exceptions are NO3 and NO5 where the relative absolute difference in $\overline{nMAE}$ is 10% and 24%, respectively. This is most likely caused by more variable cloud-cover for these locations which receive the lowest annual irradiation among all the locations in Table 1. Fig. 6(b) shows the $nMAE$ and $nMBE$ for the day-ahead ECMWF forecast. The mean value among the locations for the day-ahead market

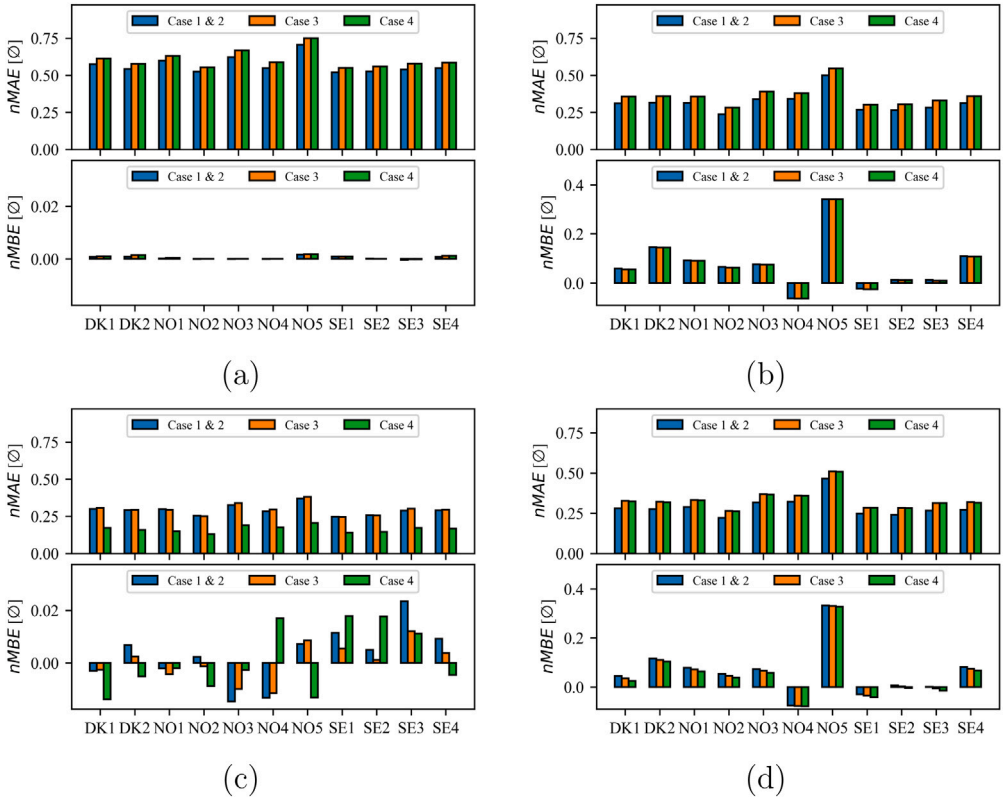

Fig. 6. Mean absolute error $nMAE$ and normalized mean bias error $nMBE$ normalized to the mean energy generation for the forecasted energy generation from the PV power plants with the smart persistence method during the period 2017–2021 on the day-ahead (a) and intraday (c) markets in the four different cases. (b) and (d) shows similar results with the ECMWF forecasts for the day-ahead and intraday markets, respectively.

in Case 1 and 2 is $\overline{nMAE} = 0.32$, with a range between 0.24 for NO2 and 0.51 for NO5. Thus, the relative reduction in $nMAE$ for the day-ahead ECMWF forecasts with respect to the smart persistence counterpart range between −29% for NO5 and −55% for NO2 for Case 1 and 2, and −27% for NO5 and −49% for NO2 for Case 3 and 4. For either forecast, the transition from 60 min to 15 min settlement periods causes an increase in the $nMAE$. For the period 2017–2021, the relative increase is 6% and 14% on average between the different locations from Case 1 and 2 to Case 3 with the smart persistence and ECMWF forecasts, respectively. With the smart persistence forecast, the $nMBE$ for the day-ahead forecast is very small in all the considered market cases. Comparing Fig. 6(a) and (b) reveals that the $nMBE$ is significantly larger for the ECMWF forecast than for the smart persistence forecast. For most locations, the bias of the day-ahead ECMWF forecast is positive. This is typical for many NWP models which consistently overestimate irradiance due to difficulty in forecasting clouds and the liquid water path (Incecik et al., 2019; Mathiesen et al., 2013; Urraca et al., 2018). However, Fig. 6(b) shows that for the two northernmost locations, i.e., NO4 and SE1, the bias is negative.

Comparing Fig. 6(a) and (c) shows that the $nMAE$ is lower with the intraday smart persistence forecast than with the day-ahead smart persistence forecast. For Case 1 and 2, the $\overline{nMAE} = 0.29$, and thus the relative reduction with respect to the day-ahead smart persistence forecast is −49 % on average between the different locations. Also with the intraday ECMWF forecast shown in Fig. 6(d), the $\overline{nMAE} = 0.29$ for Case 1 and 2 on average between the different locations, but in this case the relative reduction with respect to the day-ahead ECMWF forecast is only −8%. The transition from 60 min to 15 min settlement periods has little effect on the $nMAE$ for the intraday smart persistence forecast, but for the ECMWF forecast this change from Case 1 and 2 to Case 3 is associated with a relative increase of 16% in $nMAE$ on average between the locations. When Δt changes from 1.25 h to 0.25 h from Case 3 to Case 4, there is a relative reduction in $nMAE$ of −45% on average between the bidding areas with the smart persistence forecast. With the ECMWF forecast, the relative reduction in $nMAE$ between Case 3 and 4 is −1% or less for all locations. Comparing Fig. 6(a) and (c) shows that the absolute value of the $nMBE$ is generally larger for the intraday smart persistence forecast in comparison with its day-ahead counterpart. With the ECMWF forecast presented in Fig. 6(b) and (d), the absolute value of the $nMBE$ is typically lower with the intraday forecast than with the day-ahead counterpart, but we note that this is not the case for NO4 and SE1. For Case 1 and 2, the relative increase in the absolute value of the $nMBE$ for NO4 is 21% while the corresponding number is 28% for SE1. For SE2 and SE3, the absolute value of the $nMBE$ is less than 1% in both the day-ahead and intraday ECMWF forecasts. For the other locations, the average relative reduction in $nMBE$ with the intraday ECMWF forecast is −16% with respect to the day-ahead counterpart for Case 1 and 2. Excluding NO4, SE1, SE2, and SE3, the intraday ECMWF forecast for Case 3 results in an average relative reduction between the locations of −10% in $nMBE$ compared to Case 1 and 2 while the corresponding number is −21% for Case 4.

4.2. Energy generation

In Fig. 7, the modelled annual specific energy generation for the 10 MWp PV power plants are presented together with the corresponding specific income in the day-ahead market using a perfect forecast. In terms of total generated energy, 2018 is the overall best year and 2017 the worst. We note that no data is available for NO2 until January 1. 2020. The PV power plant in SE2 has the largest difference in yearly energy output of all the power plants, with a 237 MWh/MWp difference between year 2017 and 2018. The modelled PV power plants

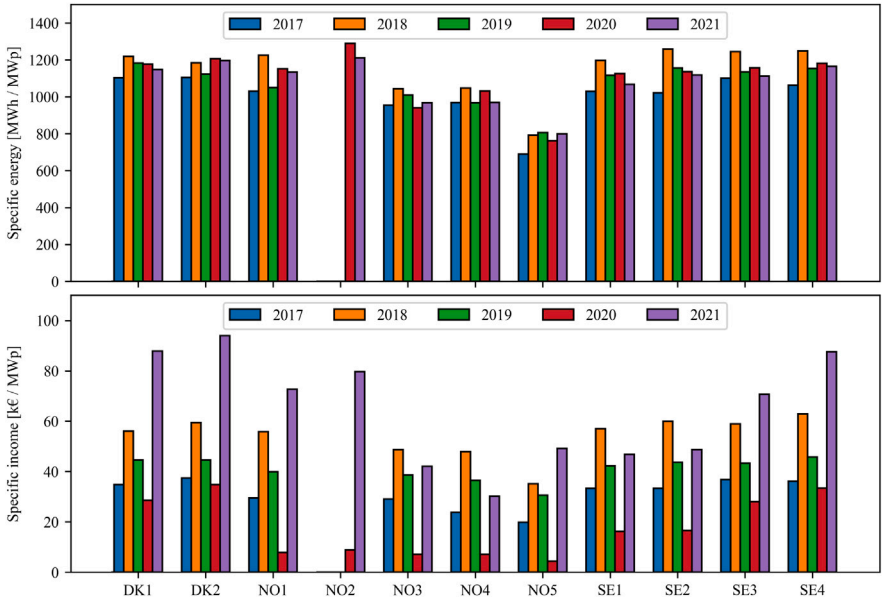

Fig. 7. In the upper figure, the annually resolved specific energy generation from the synthetic 10 MWp PV power plants is given. In the lower figure, the specific income in the day-ahead market with a perfect forecast is given. Note that with a perfect forecast, all defined market and imbalance settlement cases provide the same income. For NO2, sub-hourly irradiance data was only available for 2020 and 2021. The incomes are plotted before fixed fees, volume fees, grid tariffs and peak load reserve fees have been subtracted.

in the southernmost bidding areas, i.e., NO2, DK1, DK2 and SE4, have the overall highest energy generation. However, it should be noted that the power plants in SE1, SE2, SE3 and NO1 have only 1.4%–5.0% lower total production relative to the one in DK1 which is the highest producing PV power plant with a full record in the whole analysis period. The energy generation is lowest in NO3, NO4 and NO5 with 14.5%–33.9% lower total generation relative to that of DK1. This is expected since NO3, NO4 and NO5 receive the lowest annual irradiation among the locations in Table 1 due to cloud-cover and the high latitude of NO4.

4.3. Perfect forecast income

Despite the relatively small difference in annual generation for each individual plant, the annual income with perfect forecast has a strong yearly dependence. Over the period 2017–2021, the plant in DK2 has the highest total income of 270 k€/MWp while the one in NO5 has the lowest income with 139 k€/MWp (when neglecting the power plant in NO2 which only has data for 2020 and 2021). For the synthetic PV power plant in NO2, the estimated energy generation in 2020 is 6.4% higher than in 2021. However, the estimated income in 2020 is only 11.1% of the estimated income in 2021. As explained in Section 2.6, this is mainly caused by much precipitation and high water-levels in the hydro power reservoirs in 2020.

4.4. Market and imbalance settlement cases

In Fig. 8, the non-textured bars give the estimated income losses of the plants when bidding in the day-ahead market with the smart persistence and ECMWF forecast with respect to the income with a perfect forecast. The difference in the market-committed generation and actual generation is economically accounted for in the imbalance settlement. For Case 1, the income loss is lower in the bidding areas with large shares of hydro power capacity, i.e., all Norwegian bidding areas, as well as SE1 and SE2. This indicates that the imbalances are more expensive in the bidding areas with smaller shares of hydro power. In terms of the $nMAE$ of the day-ahead forecasts for both the smart persistence and ECMWF model, the accuracy is poorest for NO5 which could make the income loss with respect to perfect forecast larger. However, Fig. 8 demonstrates that the loss of income under Case 1 for NO5 is comparable to the other hydro-dominated bidding areas.

Interestingly, the income loss decreases significantly for all bidding areas when the single-price imbalance settlement is introduced in Case 2. This modification in the market, therefore, seems to disincentivize the need for providing more accurate forecast. The difference in the income loss in the Danish bidding areas compared to the Norwegian bidding areas are reduced for Case 2 due to the low imbalance fee in Denmark and the possibility of generating additional income from imbalances under the single-price imbalance settlement structure. E.g., when using the smart persistence forecast, the imbalance fee would have to be increased from its current value of 0.133 €/MWh to 4.20 €/MWh in order to have the same income loss in the day-ahead market for DK1 with the single-price as with the dual-price imbalance settlement structure.

When moving from 60 min to 15 min market and imbalance settlement intervals from Case 2 to Case 3 there is a negligible effect on the income losses when only trading in the day-ahead market. The synthetic PV power plants in all of the bidding areas experience higher income losses, since the costs related to the imbalance fee are cleared per quarter instead of per hour. The largest change from Case 2 to Case 3, when only bidding in the day-ahead market, is observed for NO3 where the income loss increases by less than 0.2%, or approximately 600 €/year using either the smart persistence or the ECMWF forecast.

The textured bars of Fig. 8 show the estimated income loss when participating in both the day-ahead and intraday markets. When using the smart persistence model, intraday trading is beneficial for all cases and bidding areas. As explained in Section 2.4, this is due to the smart persistence forecast accuracy increasing in the intraday market compared to the day-ahead market, and less extreme prices in the intraday market compared to the regulating market. However, even though the $nMAE$ for the ECMWF model is lower for the intraday compared to the day-ahead forecasts for all modelled PV power plants, the income losses both increase and decrease with intraday trading. This indicates that the imbalances of the ECMWF model achieve better prices in the regulating market compared to the intraday market for some of the bidding areas. In addition, under Case 2–4, if the imbalances help

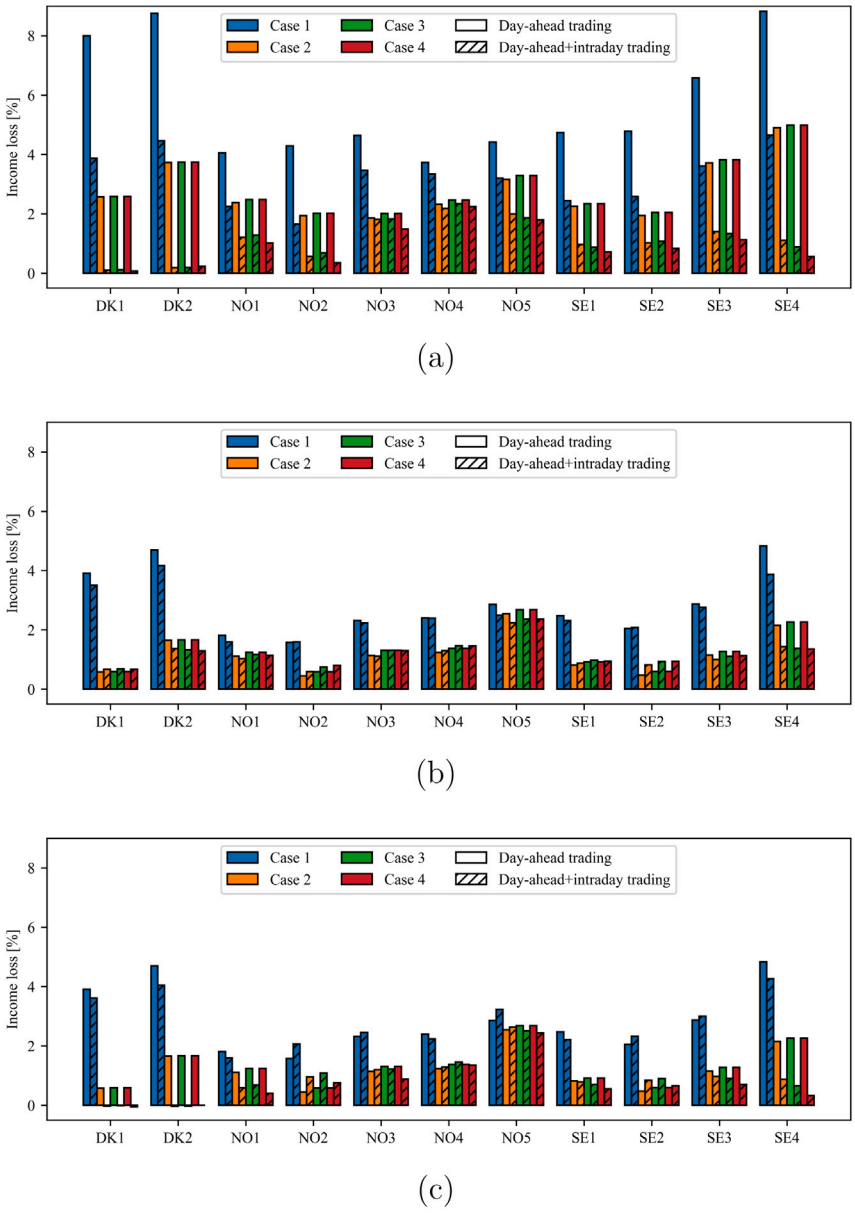

Fig. 8. The relative income loss with respect to the income with a perfect forecast for the defined energy market and imbalance settlement cases using historical market data from 2017 throughout 2021. Note that for NO2, data is only available for 2020 and 2021. In (a) and (b), the smart persistence and ECMWF forecasts are used respectively for both the day-ahead and intraday markets. In (c), the ECMWF forecast is used for the day-ahead market, and the smart persistence forecast for the intraday market.

the total energy system being in balance, the imbalances can provide additional revenues, i.e., reducing the income losses. Thus, clearing them through the intraday market is not always beneficial.

When participating in both the day-ahead and intraday market, the income losses can either increase or decrease depending on the bidding area when comparing Case 2 with Case 3. Thus, the results show that the incentive to improve the forecast is not greater when clearing the markets and imbalance settlements on 15 min instead of 60 min intervals under the single-price imbalance settlement structures. With the smart persistence forecast, the income loss is smaller for all bidding areas in Case 4 than in Case 3, except for DK2, as the intraday gate closure is moved closer to delivery. Thus, for the PV power plants using the smart persistence forecast in their close to delivery intraday trading, their self-regulation and imbalance penalty prevention could be increased if this change is implemented in the Scandinavian energy market. With increased forecast accuracy, the TSOs' requirement to provide reserves could be decreased if the gate closure of the intraday market is extended closer to delivery, as found in Kaur et al. (2016).

In Fig. 8(c), the ECMWF forecast is used for the day-ahead market, and the smart persistence for the intraday market. Compared to only using the smart persistence or ECMWF forecasts, the income losses either increase or decrease depending on the market cases and bidding areas. However, since the strategy of combining the forecasts provides the lowest total imbalance volumes, it relates to lower risk of high income losses in the imbalance settlement. Under the combined forecast strategy, DK1 and DK2 can achieve higher income than a perfect day-ahead forecast would provide. This is because producer imbalances can generate additional income if counteracting the system imbalances in the single-price imbalance settlement structure, as explained in Section 2.5. This suggests that if the PV producers could forecast when the energy system would need up- or down-regulation, the market bids could be adjusted accordingly to maximize the profits, as also found by Pierro et al. (2020). However, if this market speculation increases

the net imbalances, it would breach the contract between the BRP and eSett which states the BRPs must aim for being in balance (eSett, 2022b).

Under the present and future market cases, i.e., Case 2, 3 and 4, considering both day-ahead and intraday trading, the income losses relative to perfect forecast range between: (i) 0.1 and 2.3% using only the smart persistence model; (ii) 0.6 and 2.4% for only the ECMWF model; and (iii) −0.1 and 2.6% with the combined forecast strategy. As the income losses vary greatly between the bidding areas, producers should note in which bidding area their PV power plants are located before taking measures to increase their forecast accuracy, as the smart persistence forecast is sufficient to ensure low income losses in the imbalance settlement for some bidding areas. E.g. for the Danish bidding areas, using the smart persistence forecast for the day-ahead and intraday trading only provide income losses up to 0.3% in Case 2–4. This implies that the imbalance fee is so low that the producers have no incentive to improve the forecast technique beyond the smart persistence forecast.

Since most of the PV power plants benefit from intraday trading, and since the $nMAE$ for both forecasting methods is lower for the intraday compared to the day-ahead forecast for all cases and PV power plants, it is likely that the traded volumes in the intraday market will increase with the amount of intermittent renewables in the electricity mix. This is indeed seen in DK1 and DK2, where there are many VRE units and intraday trading is prevalent (see Fig. A.1 in Appendix). In addition, increased generation from VRE units could increase the need for regulating power due to the uncertainty of the scheduling. Under the single-price imbalance settlement the TSOs can incentivize the power plants to provide more accurate forecasts, and thus, less imbalances, by increasing the imbalance fees. Higher imbalance fees will further incentivize self-regulation in the intraday market.

5. Conclusion

The present work has explored the value of forecasts issued for PV power plants in the Scandinavian energy markets. The energy generation from 11 synthetic PV power plants with 10 MWp installed capacity were modelled in each of the 11 Scandinavian bidding areas using sub-hourly global horizontal irradiance, ambient temperature and wind speed data from 2017 throughout 2021. Forecasts were generated by the smart persistence model and a state-of-the-art NWP model from ECMWF. Using historical energy market data, the income in the day-ahead and intraday markets under the past, present and future Scandinavian market and imbalance settlement structures was estimated based on the issued forecasts.

When bidding in the day-ahead markets, the ECMWF forecast is more accurate than the smart persistence forecast. For the intraday market, both forecast models achieve higher accuracy, but when clearing the markets on 15 min intervals the smart persistence forecast has a higher accuracy than the ECMWF forecast which is only issued twice a day. In addition, extending the intraday gate closure until the start of the settlement periods increases the intraday forecast accuracy for both forecasting models.

The modelled PV power plants in the southernmost locations, i.e., DK1, DK2, NO2 and SE4, have the highest annual energy generation of 1.2 MWh/kWp on average. The income is also the highest for these locations, but the annual income is highly dependent on the annual precipitation and reservoir water-levels due to the large shares of hydro power in the region.

The ECMWF forecast provides less income losses than the smart persistence forecast when only participating in the day-ahead market. However, when operating in both the day-ahead and intraday market for the current and future market and imbalance settlements (Case 2–4), the income losses when only using the smart persistence model were in range of the losses using the ECMWF forecast. In this regard, the income losses relative to having perfect day-ahead forecasts ranged between: (i) 0.1 and 2.3% for the smart persistence model; (ii) 0.6 and 2.4% for the ECMWF model; and (iii) −0.1 to 2.6% when using the ECMWF model for the day-ahead forecast and the smart persistence model for the intraday forecast. These ranges corresponds to the income losses producers operating in the Scandinavian markets should consider when having a single PV power plant in their portfolio for a given bidding area.

Our results demonstrate that the value of providing accurate forecasts is significantly larger under the abolished dual — than the new single-price imbalance settlement structure. In addition, moving from 60 min to 15 min settlement periods under the single-price imbalance settlement seems to have little effect on the forecast values. Generally, when using the smart persistence model for the intraday forecasts, trading in the intraday market decreases the imbalance costs, providing incentives for PV producers to do so. If the gate closure of the intraday trades would be extended until the start of the settlement period, the market and imbalance settlement structure would ensure that the PV producers could minimize their total imbalance and related costs at the same time, providing value both for themselves and the TSOs. Moreover, the TSOs could ensure higher value for more accurate forecasts in the Scandinavian energy markets by increasing the imbalance fees from their current values.

Based on the presented results, the authors advice power producers in the Scandinavian markets to use a NWP model for their day-ahead forecasts and trading forecasted imbalances in the intraday market using a short-range forecasting method, i.e., the smart persistence model. Future work should assess the PV forecast value for producers with multiple generation technologies in their portfolio, since some of the PV imbalances could be compensated for by imbalances of opposite direction from other VRE power plants. Furthermore, future work should calculate the investment and operating costs of implementing different forecasting methods and compare these costs to the forecast values, i.e. the saved income losses in the imbalance settlement, to assess the economic feasibility of the forecasting methods. Power producers in other markets should also investigate the forecast value for their specific market and imbalance settlement structures in order to assess if investing in sophisticated forecasting methods is economically beneficial or not.

Declaration of competing interest

The authors declare that they have no known competing financial interests or personal relationships that could have appeared to influence the work reported in this paper.

Acknowledgements

The authors acknowledge funding from the Research Council of Norway (KSP HydroSun, grant no. 328640). Anne Gerd Imenes is acknowledged for granting access to measurements of global horizontal irradiance carried out at the University of Agder (UiA). Thomas Carlund of the Swedish Meteorological and Hydrological Institute (SMHI) is acknowledged for granting access to measurements of global horizontal irradiance carried out in Sweden. The authors would also acknowledge representatives from Nord Pool, eSett, Statnett, Sira Kvina and Agder Energi for answering inquiries related to this study.

Appendix

See Table A.1, Table A.2 and Fig. A.1.

Table A.1
Descriptive statistics of the difference between the average intraday prices and day-ahead prices from 2017 throughout 2021, only considering hours with historical intraday trades. IQR is the interquartile range defined as $IQR = Q_3 - Q_1$ where Q_1 and Q_3 are the first and third quartile of the dataset, respectively.

Bid.area	Min [€/MWh]	Q_1 [€/MWh]	Median [€/MWh]	Q_3 [€/MWh]	Max [€/MWh]	IQR [€/MWh]
DK1	−156.73	−4.11	−0.89	1.84	499.24	5.95
DK2	−190.46	−3.23	−0.39	2.27	530.38	5.50
NO1	−162.63	−3.23	−0.21	1.78	185.38	5.01
NO2	−109.09	−3.24	−0.06	2.43	214.00	5.67
NO3	−152.50	−2.65	−0.10	1.87	205.38	4.52
NO4	−90.57	−2.81	−0.06	2.40	150.40	5.21
NO5	−164.26	−2.29	0.69	4.10	176.75	6.39
SE1	−98.58	−2.62	−0.37	1.15	337.93	3.77
SE2	−120.11	−2.80	−0.55	1.47	206.65	4.27
SE3	−128.99	−2.79	−0.51	1.47	304.91	4.26
SE4	−150.34	−3.00	−0.33	1.89	272.02	4.89

Table A.2
Descriptive statistics of the difference between the single regulating prices and day-ahead prices from 2017 throughout 2021. The single regulating prices were constructed from the historical dual regulating prices. IQR is the interquartile range defined as $IQR = Q_3 - Q_1$ where Q_1 and Q_3 are the first and third quartile of the dataset, respectively.

Bid.area	Min [€/MWh]	Q_1 [€/MWh]	Median [€/MWh]	Q_3 [€/MWh]	Max [€/MWh]	IQR [€/MWh]
DK1	−410.09	−5.19	0.00	0.13	1826.82	5.32
DK2	−410.09	−5.37	0.00	1.38	718.64	6.47
NO1	−390.25	−4.05	0.00	1.62	675.00	5.67
NO2	−390.25	−4.03	0.00	1.58	675.00	5.61
NO3	−218.52	−4.49	0.00	0.88	4875.19	5.37
NO4	−218.52	−3.99	0.00	0.00	4875.19	3.99
NO5	−390.25	−4.00	0.00	1.67	675.00	5.67
SE1	−1001.77	−5.14	0.00	0.50	4875.19	5.64
SE2	−1001.77	−5.14	0.00	0.50	4875.19	5.64
SE3	−1001.77	−4.73	0.00	1.58	4834.51	6.31
SE4	−1001.77	−5.06	0.00	1.42	4834.51	6.48

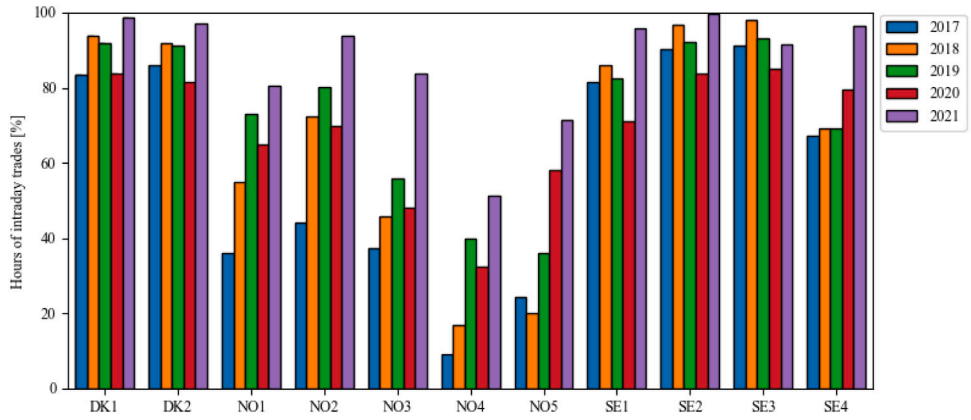

Fig. A.1. The percentage of the hours with intraday trades in each year and bidding area. Bars with 100% hours of intraday trades had historical intraday trades for each hour in the given year.

References

All NEMO Committee, 2022a. About the all NEMO committee. https://www.nemo-committee.eu/nemo_committee. (Accessed 05 August 2022).

All NEMO Committee, 2022b. Single day-ahead coupling (SDAC). https://www.nemo-committee.eu/sdac. (Accessed 05 August 2022).

All NEMO Committee, 2022c. Single intraday coupling (SIDC). https://www.nemo-committee.eu/sidc. (Accessed 08 August 2022).

Antonanzas, J., Osorio, N., Escobar, R., Urraca, R., de Pison, F.M., Antonanzas-Torres, F., 2016. Review of photovoltaic power forecasting. Sol. Energy 136, 78–111. http://dx.doi.org/10.1016/j.solener.2016.06.069, URL: https://www.sciencedirect.com/science/article/pii/S0038092X1630250X.

Antonanzas, J., Pozo-Vázquez, D., Fernandez-Jimenez, L.A., de Pison, F.J.M., 2017. The value of day-ahead forecasting for photovoltaics in the spanish electricity market. Sol. Energy 158, 140–146. http://dx.doi.org/10.1016/j.solener.2017.09.043.

Chu, Y., Li, M., Coimbra, C.F., Feng, D., Wang, H., 2021. Intra-hour irradiance forecasting techniques for solar power integration: A review. iScience 24 (10), 103136. http://dx.doi.org/10.1016/j.isci.2021.103136, URL: https://www.sciencedirect.com/science/article/pii/S2589004221011044.

De Giorgi, M.G., Congedo, P.M., Malvoni, M., Laforgia, D., 2015. Error analysis of hybrid photovoltaic power forecasting models: A case study of mediterranean climate. Energy Convers. Manage. 100, 117–130. http://dx.doi.org/10.1016/j.enconman.2015.04.078, URL: https://www.sciencedirect.com/science/article/pii/S0196890415004422.

Dobos, A.P., 2014. PVWatts Version 5 Manual. Technical Report, National Renewable Energy Lab.(NREL), Golden, CO (United States).

Energiforsk, 2021. EL FRÅN NYA ANLÄGGNINGAR.

ENTSO-E Transparency Platform, 2022. Actual generation per production type. http://transparency.entsoe.eu/generation/r2/actualGenerationPerProductionType/show. (Accessed 08 August 2022).

eSett, 2022a. Fees. https://opendata.esett.com/fees_1tase. (Accessed 08 August 2022).

eSett, 2022b. Nordic imbalance settlement handbook instructions and rules for market participants 2nd of may 2022. https://www.esett.com/handbook/. (Accessed 08 August 2022).

eSett, 2022c. Nordic imbalance settlement handbook instructions and rules for market participants 7th of december 2020. Personal Communications. 07.04.2022.

EU Science Hub, 2022. Photovoltaic geographical information system. https://re.jrc.ec.europa.eu/pvg_tools/en/. (Accessed 23 August 2022).

Faiman, D., 2008. Assessing the outdoor operating temperature of photovoltaic modules. Prog. Photovolt., Res. Appl. 16 (4), 307–315.

Fosso, O., Gjelsvik, A., Haugstad, A., Mo, B., Wangensteen, I., 1999. Generation scheduling in a deregulated system. The Norwegian case. IEEE Trans. Power Syst. 14 (1), 75–81. http://dx.doi.org/10.1109/59.744487.

Holmgren, W.F., Hansen, C.W., Mikofski, M.A., 2018. pvlib python: A python package for modeling solar energy systems. J. Open Source Softw. 3 (29), 884.

IEA, 2014. The power of transformation. https://www.iea.org/reports/the-power-of-transformation. (Accessed 08 August 2022).

Incecik, S., Sakarya, S., Tilev, Ş., Kahraman, A., Aksoy, B., Çalışkan, E., Topcu, S., Kahya, C., Odman, M., 2019. Evaluation of WRF parameterizations for global horizontal irradiation forecasts: A study for Turkey. Atmosfera 32, 143–158. http://dx.doi.org/10.20937/ATM.2019.32.02.05.

Ineichen, P., Perez, R., 2002. A new airmass independent formulation for the Linke turbidity coefficient. Sol. Energy 73 (3), 151–157.

Kaur, A., Nonnenmacher, L., Pedro, H.T., Coimbra, C.F., 2016. Benefits of solar forecasting for energy imbalance markets. Renew. Energy 86, 819–830. http://dx.doi.org/10.1016/j.renene.2015.09.011, URL: https://www.sciencedirect.com/science/article/pii/S0960148115302901.

Long, C.N., Dutton, E.G., 2010. BSRN Global Network Recommended QC Tests, V2. x. PANGAEA.

Luoma, J., Mathiesen, P., Kleissl, J., 2014. Forecast value considering energy pricing in California. Appl. Energy 125, 230–237. http://dx.doi.org/10.1016/j.apenergy.2014.03.061.

Marquez, R., Coimbra, C.F., 2013. Proposed metric for evaluation of solar forecasting models. J. Sol. Energy Eng. 135 (1).

Mathiesen, P., Collier, C., Kleissl, J., 2013. A high-resolution, cloud-assimilating numerical weather prediction model for solar irradiance forecasting. Sol. Energy 92, 47–61. http://dx.doi.org/10.1016/j.solener.2013.02.018, URL: https://www.sciencedirect.com/science/article/pii/S0038092X13000832.

Maxwell, E.L., 1987. A Quasi-Physical Model for Converting Hourly Global Horizontal to Direct Normal Insolation. Technical Report, Solar Energy Research Inst., Golden, CO (USA).

Micic, I., 2022. Day-ahead markets. In: The Physical and Financial Power Markets. Nord Pool Academy.

NBM, 2022. Nordic balancing model. https://nordicbalancingmodel.net/. (Accessed 05 August 2022).

Nord Pool, 2022a. Bidding areas. https://www.nordpoolgroup.com/en/the-power-market/Bidding-areas/. (Accessed 05 August 2022).

Nord Pool, 2022b. Market data. https://www.nordpoolgroup.com/en/Market-data1/#/nordic/table. (Accessed 05 August 2022).

Nord Pool, 2022c. Price coupling of regions (PCR). https://www.nordpoolgroup.com/en/the-power-market/Day-ahead-market/Price-coupling-of-regions/. (Accessed 05 August 2022).

Perez, R., Ineichen, P., Seals, R., Michalsky, J., Stewart, R., 1990. Modeling daylight availability and irradiance components from direct and global irradiance. Sol. Energy 44 (5), 271–289.

Perez, R., Seals, R., Ineichen, P., Stewart, R., Menicucci, D., 1987. A new simplified version of the Perez diffuse irradiance model for tilted surfaces. Sol. Energy 39 (3), 221–231.

Perez, R., Stewart, R., Seals, R., Guertin, T., 1988. The Development and Verification of the Perez Diffuse Radiation Model. Technical Report, Sandia National Lab.(SNL-NM), Albuquerque, NM (United States); State Univ ....

Persson, A., Grazzini, F., 2007. User guide to ECMWF forecast products. Meteorol. Bull. 3, 2.

Pierro, M., Moser, D., Perez, R., Cornaro, C., 2020. The value of PV power forecast and the paradox of the "single pricing" scheme: The Italian case study. Energies 13, http://dx.doi.org/10.3390/en13153945.

Sobri, S., Koohi-Kamali, S., Rahim, N.A., 2018. Solar photovoltaic generation forecasting methods: A review. Energy Convers. Manage. 156, 459–497. http://dx.doi.org/10.1016/j.enconman.2017.11.019, URL: https://www.sciencedirect.com/science/article/pii/S0196890417310622.

Spodniak, P., Ollikka, K., Honkapuro, S., 2021. The impact of wind power and electricity demand on the relevance of different short-term electricity markets: The nordic case. Appl. Energy 283, http://dx.doi.org/10.1016/j.apenergy.2020.116063.

Statnett, 2022a. 15 Minutters avregning og energimarkeder. https://www.statnett.no/for-aktorer-i-kraftbransjen/systemansvaret/kraftmarkedet/15-minutters-avregning-og-energimarkeder/. (Accessed 05 August 2022).

Statnett, 2022b. Personal communications. 09.05.2022.

Svenska kraftnät, 2022. Produktionsstatistik. https://mimer.svk.se/ProductionConsumption/ProductionIndex. (Accessed 08 August 2022).

Urraca, R., Huld, T., Gracia-Amillo, A., de Pison, F.J.M., Kaspar, F., Sanz-Garcia, A., 2018. Evaluation of global horizontal irradiance estimates from ERA5 and COSMO-REA6 reanalyses using ground and satellite-based data. Sol. Energy 164, 339–354. http://dx.doi.org/10.1016/j.solener.2018.02.059, URL: https://www.sciencedirect.com/science/article/pii/S0038092X18301920.

Wang, Y., Millstein, D., Mills, A.D., Jeong, S., Ancell, A., 2022. The cost of day-ahead solar forecasting errors in the United States. Sol. Energy 231, 846–856. http://dx.doi.org/10.1016/j.solener.2021.12.012.

WMO, 2019. General Meteorological Standards and Recommended Practices. Basic Documents No. 2, WMO–No. 49, World Meteorological Organization Geneva.